




Article

PI3K/AKT/ β -Catenin Signaling Regulates Vestigial-Like 1 Which Predicts Poor Prognosis and Enhances Malignant Phenotype in Gastric Cancer

Bo-Kyung Kim ^{1,†,*} , Jae-Ho Cheong ^{2,3,†}, Joo-Young Im ¹ , Hyun Seung Ban ⁴ ,
Seon-Kyu Kim ¹, Mi-Jung Kang ¹, Jungwoon Lee ⁵, Seon-Young Kim ^{1,6}, Kyung-Chan Park ^{1,6},
Soonmyung Paik ³ and Misun Won ^{1,6,*}

¹ Personalized Genomic Medicine Research Center, KRIBB, Daejeon 34141, Korea; imjy@kribb.re.kr (J.-Y.I.); seonkyu@kribb.re.kr (S.-K.K.); kmj87@kribb.re.kr (M.-J.K.); kimsy@kribb.re.kr (S.-Y.K.); kpark@kribb.re.kr (K.-C.P.)

² Department of Surgery, Yonsei University College of Medicine, Seoul 03722, Korea; JHCHEONG@yuhs.ac.kr

³ Severance Biomedical Science Institute, Yonsei University College of Medicine, Seoul 03722, Korea; SOONMYUNGPAIK@yuhs.ac.kr

⁴ Biotherapeutics Translational Research Center, KRIBB, Daejeon 34141, Korea; banhs@kribb.re.kr

⁵ Immunotherapy Convergence Research Center, KRIBB, Daejeon 34141, Korea; jwlee821@kribb.re.kr

⁶ KRIBB School of Bioscience, Korea University of Science and Technology, Daejeon 34113, Korea

* Correspondence: kimbk@kribb.re.kr (B.-K.K.); misun@kribb.re.kr (M.W.); Tel.: +82-42-879-8177 (B.-K.K.); +82-42-860-4178 (M.W.)

† These authors contribute equally to this work.

Received: 25 October 2019; Accepted: 29 November 2019; Published: 3 December 2019



Abstract: Although gastric cancer is a common cause of cancer mortality worldwide, its biological heterogeneity limits the available therapeutic options. Therefore, identifying novel therapeutic targets for developing effective targeted therapy of gastric cancer is a pressing need. Here, we investigate molecular function and regulatory mechanisms of *Vestigial-like 1* (*VGLL1*) in gastric cancer. Microarray analysis of 556 gastric cancer tissues revealed that *VGLL1* was a prognostic biomarker that correlated with *PI3KCA* and *PI3KCB*. *VGLL1* regulates the proliferation of gastric cancer cells, as shown in live cell imaging, sphere formation, and in vivo xenograft model. Tail vein injection of NUGC3 cells expressing sh*VGLL1* resulted in less lung metastasis occurring when compared to the control. In contrast, larger metastatic lesions in lung and liver were detected in the *VGLL1*-overexpressing NUGC3 cell xenograft excision mouse model. Importantly, *VGLL1* expression is transcriptionally regulated by the PI3K-AKT- β -catenin pathway. Subsequently, *MMP9*, a key molecule in gastric cancer, was explored as one of target genes that were transcribed by *VGLL1*-TEAD4 complex, a component of the transcription factor. Taken together, PI3K/AKT/ β -catenin signaling regulates the transcription of *VGLL1*, which promotes the proliferation and metastasis in gastric cancer. This finding suggests *VGLL1* as a novel prognostic biomarker and a potential therapeutic target.

Keywords: gastric cancer; *MMP9*; PI3K; *VGLL1*

1. Introduction

Gastric cancer is biologically heterogeneous and it presents various genetic alterations. Most gastric cancer patients are diagnosed at an advanced stage, and conventional chemotherapy has shown limited efficacy. A recent report predicted the prognosis and response to adjuvant chemotherapy in gastric cancer patients by classifying individuals based on cancer-related genes [1]. Although significant efforts have been made for targeted molecular therapies, only a few targeted therapies that extend

survival are currently available for patients with gastric cancer. The majority of these patients exhibit resistance while the monoclonal anti-HER2 antibody Trastuzumab is effective in some *HER*-positive gastric cancer patients [2–4]. Ramucirumab, which is an antibody that targets VEGFR-2, has proven to be useful alone or in combination with paclitaxel as a second-line treatment for advanced gastric cancer [5,6]. To date, the gastric cancer-related potential therapeutic targets include EGFR, VEGF, MET, FGFR, PI3K/mTOR, and HDAC [5,7,8]. Unfortunately, clinical trials for inhibitors of these identified targets have failed to demonstrate significant clinical efficacy [5,6]. Therefore, there is a critical need to identify novel therapeutic targets based on the molecular mechanisms of gastric cancer.

The Cancer Genome Atlas classifies gastric cancer into four types based on genetic changes [9,10]. Somatic mutations, such as amplification, deletions, and structural abnormalities in chromosomal region, TP53 mutations, and amplification of the RTK/RAS/MAPK pathway characterize the chromosomal instability (CIN) subtype. Genomically stable (GS) subtype, which is associated with diffuse gastric cancer, has frequently mutations in *RHOA* and *CDH1* gene or fusions involving Rho-family GTPase-activating proteins (GAP). The microsatellite instability (MSI) subtype is characterized by *PI3KCA*, *ERBB3*, and *MLH1* silencing, MHC class 1 gene alterations, and tumor-specific neoantigens. The Epstein-Barr virus (EBV) subtype has a high rate of *PI3KCA* mutations and high *PD-L1/L2* expression. *PI3KCA* mutation frequently occurs in 80% of EBV subtype tumors and 3% of CIN subtype tumors [11]. The mutation or amplification of *PI3KCA* and *PI3KCB* promotes cell growth and drug resistance [12,13].

The *Vestigial-like* (*VGLL*) family that comprises *VGLL1-4* is named after the *Drosophila* transcriptional coactivator Vestigial (Vg) [14]. They contain the TOUDU domain to mediate interactions with TEA domain transcription factors (TEADs), which are essential in development [14,15]. *TEAD4*, which is a member of the Hippo signaling pathway, is overexpressed in various cancers and it requires coactivators, such as Yes-associated protein (*YAP*) or transcription coactivator with a PDZ-binding motif (*TAZ*) to induce the expression of *c-myc*, *Axl*, *survivin*, *CTGF*, *cyr61*, and *VEGF-A* [15–17]. *VGLL4* functions as a tumor suppressor in cancer by competing with *YAP* for TEAD binding [18–20]. Interestingly, the structural similarities between *VGLL1* and *YAP* or *TAZ* suggest the formation of the *VGLL1*–TEAD complex [21,22]. *VGLL1* expression is reported to be associated with reduced overall survival (OS) in triple-negative basal-like breast carcinoma [23]. However, the molecular function of *VGLL1* in cancer remains unclear.

Here, we investigated the clinical relevance and molecular function of *VGLL1* in gastric cancer through in vitro experiments and in vivo mouse models. We further explored the underlying regulatory mechanisms for evaluating *VGLL1* as a potential therapeutic target in gastric cancer

2. Results

2.1. *VGLL1* Is a Novel Prognostic Biomarker Correlated with *PI3KCA* in Gastric Cancer

We assessed the clinical relevance of *VGLL1* in gastric cancer by immunohistochemistry (IHC) of gastric cancer specimens. In adenocarcinoma tissues, *VGLL1* expression was 55% higher when compared to healthy tissues (Figure 1a). *VGLL1* expression was high in NUGC3, NCI-N87, SNU16, SNU216, and MKN28 cells (Figure 1b), but it was barely detectable in SNU5, SNU484, SNU668, and Hs746T cells.

Next, we performed microarray analyses of specimens from 556 gastric cancer patients to understand the clinical relevance of *VGLL1* [1]. The overall survival (OS) and recurrence-free survival (RFS) rates were lower in the *VGLL1*-high subgroup than in the *VGLL1*-low subgroup (Figure 1c,d). The high expression of *VGLL1* was significantly associated with Lauren classification, primary tumor (pT), malignancy (TNM), and lymphatic invasion status (Supplementary Table S1). These results indicated positive correlations between *VGLL1* expression and the clinicopathological parameters in gastric cancer patients.

We explored 172 genes in the subgroup with high VGLL1 expression to gain insights into the role of VGLL1 in gastric cancer. Gene Ontology analysis suggested the significance of phosphatidylinositol 3 kinase signaling, phosphatidylinositol-3-phosphate biosynthetic processes, phosphatidylinositol phosphate kinase activity, and 1-phosphatidylinositol-4-phosphate-3-kinase activity (Figure 1e,f). VGLL1 expression was positively correlated with PIK3CA and PIK3CB, which are associated with poor OS in gastric cancer patients (Figure 1g,h).

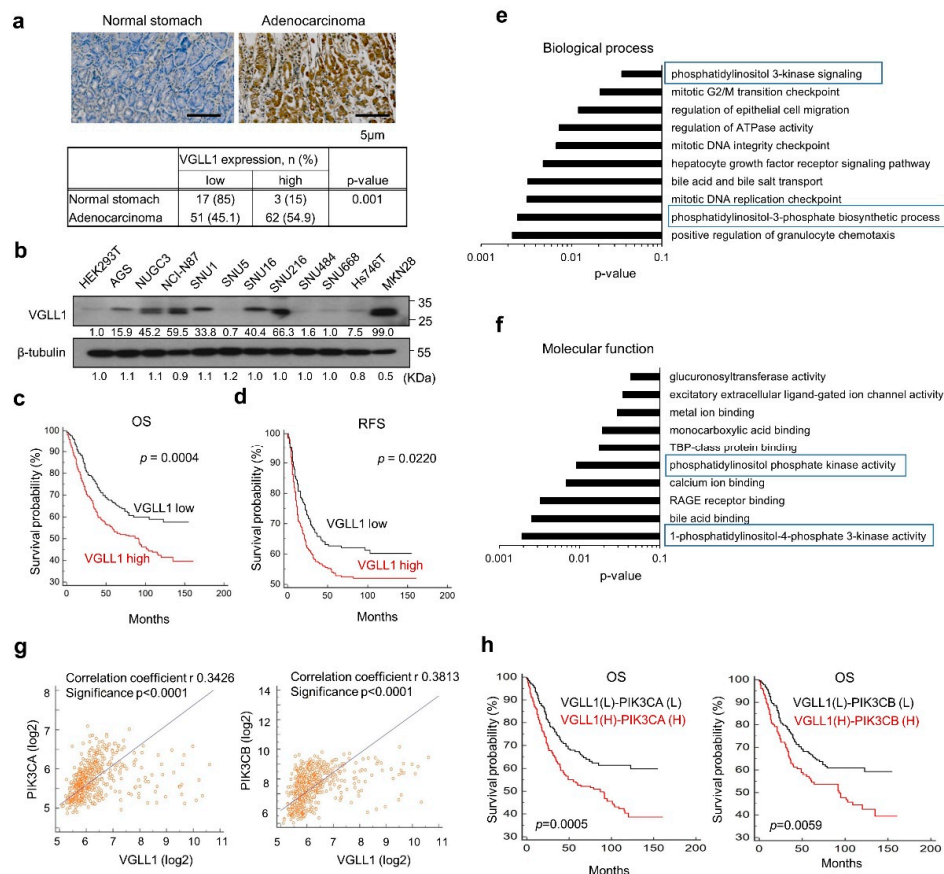


Figure 1. Vestigial-like 1 (VGLL1) expression is correlated with gastric cancer and PI3K. **(a)** VGLL1 expression in gastric cancer. Representative IHC images of normal and gastric cancer tissue samples (original magnification: 200 \times). Scale bar: 5 μ m. Chi-squared test. **(b)** VGLL1 expression in human gastric cancer cell lines was analyzed using western blotting. **(c,d)** Kaplan-Meier curves of overall survival (OS) and recurrence-free survival (RFS) in gastric cancer patients stratified by VGLL1 expression. Survival curves were compared using Log rank test. **(e,f)** In Microarray analysis of 556 patients with gastric cancer, 202 genes were up-regulated in VGLL1 high subgroup compared to VGLL1 low subgroups (FDR correction, p value < 0.05 and $\log_2FC > 1$). For Gene Ontology analysis of the 202 genes, classification enrichment was determined while using the DAVID tool. **(g)** Pearson correlations between VGLL1 and PIK3CA or PPIK3CB in gastric cancer patients. **(h)** Kaplan-Meier curves of gastric cancer patient subgroups defined by their combination of VGLL1 and PIK3CA or PPIK3CB expression levels.

2.2. VGLL1 Regulates the Proliferation of Gastric Cancer Cells

We examined the effect of VGLL1 expression on cell proliferation to understand the VGLL1 function. VGLL1 knockdown inhibited the growth of NUGC3, AGS, and NCI-N87 cells (Figure 2a; Supplementary Figure S1b), whereas VGLL1 overexpression enhanced the growth of NUGC3, AGS, HEK293T, SNU484, SNU638, and SNU668 cells (Figure 2b; Supplementary Figures S1c and S2). In a spheroid culture assay, NUGC3 cells stably overexpressing VGLL1 formed larger spheroids

than those of the control cells (Figure 2c). In vivo tumor formation of NUGC3 cells expressing VGLL1-specific shRNAs was significantly reduced when compared to the control (Figure 2d). However, the VGLL1-overexpressing HEK293T cells formed larger tumors than the control cells (Figure 2e). Although HEK293T are not gastric cancer cells, these results are suggestive, but they do not prove that VGLL1 is important for the increased proliferation of xenografts.

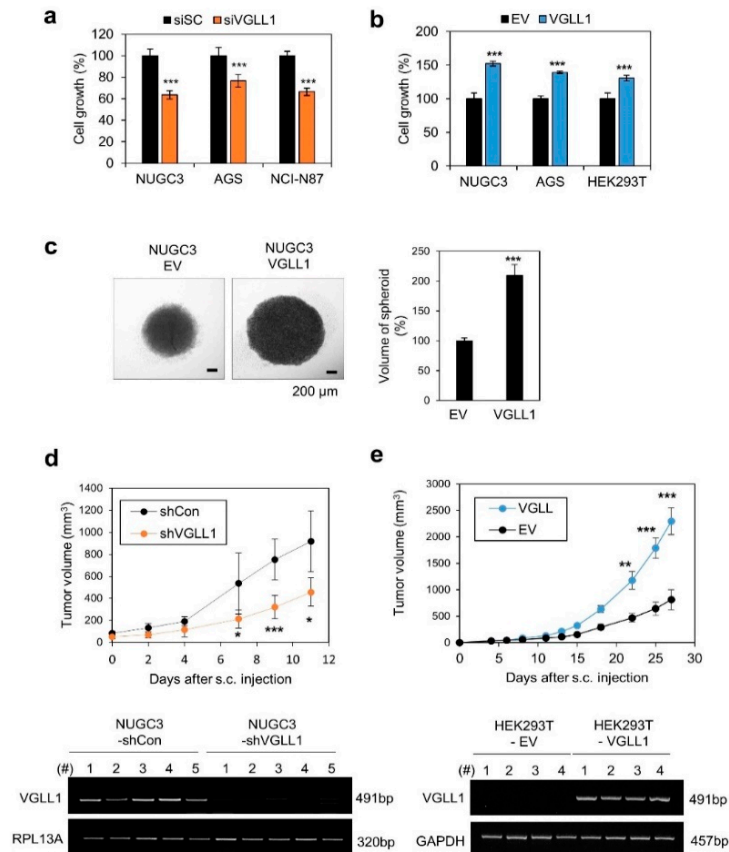


Figure 2. VGLL1 is involved in gastric cancer cell proliferation. (a,b) Effect of VGLL1 expression knockdown (a) or overexpression (b) on cell growth measured by live-cell imaging. $n = 4$; *** $p < 0.005$ (Student's *t*-test). (c) Effect of VGLL1 overexpression on spheroid formation in stable VGLL1-overexpressing NUGC3 (NUGC3-VGLL1) and control (NUGC3-Empty Vector) cells. $n = 5$; *** $p < 0.005$ (Student's *t*-test). (d) In vivo tumor formation of NUGC3 cells infected with Lenti-shVGLL1 or Lenti-shControl. (e) In vivo tumor formation of VGLL1-overexpressing HEK293T cells. VGLL1 expression in tumor tissues of the xenograft model as measured by RT-PCR. * $p < 0.05$, ** $p < 0.01$, *** $p < 0.005$ (Student's *t*-test).

2.3. VGLL1 Regulates Metastasis of Gastric Cancer Cells in *In Vitro* and *In Vivo* Mouse Models

We then investigated the role of VGLL1 in cancer metastasis. In a migration assay, NUGC3 cells that were treated with shVGLL1 migrated more slowly than the control cells, whereas VGLL1-overexpressing NUGC3 cells migrated faster than the control cells (Figure 3a). Moreover, the invasiveness of VGLL1-overexpressing NUGC3 cells significantly exceeded that of the control cells (Figure 3b). In an *in vivo* mouse model, tail vein injection of NUGC3 cells expressing shVGLL1 resulted in fewer lung metastasis, whereas bigger nodules and a larger metastatic area were found in the lungs of mice expressing the shControl (Figure 3c). Furthermore, metastatic lesions were detected by H&E staining and Ki67 IHC in the lungs and liver in a xenograft model with VGLL1-overexpressing NUGC3 cells (Figure 3d). These results suggest that VGLL1 plays a crucial role in gastric cancer metastasis.

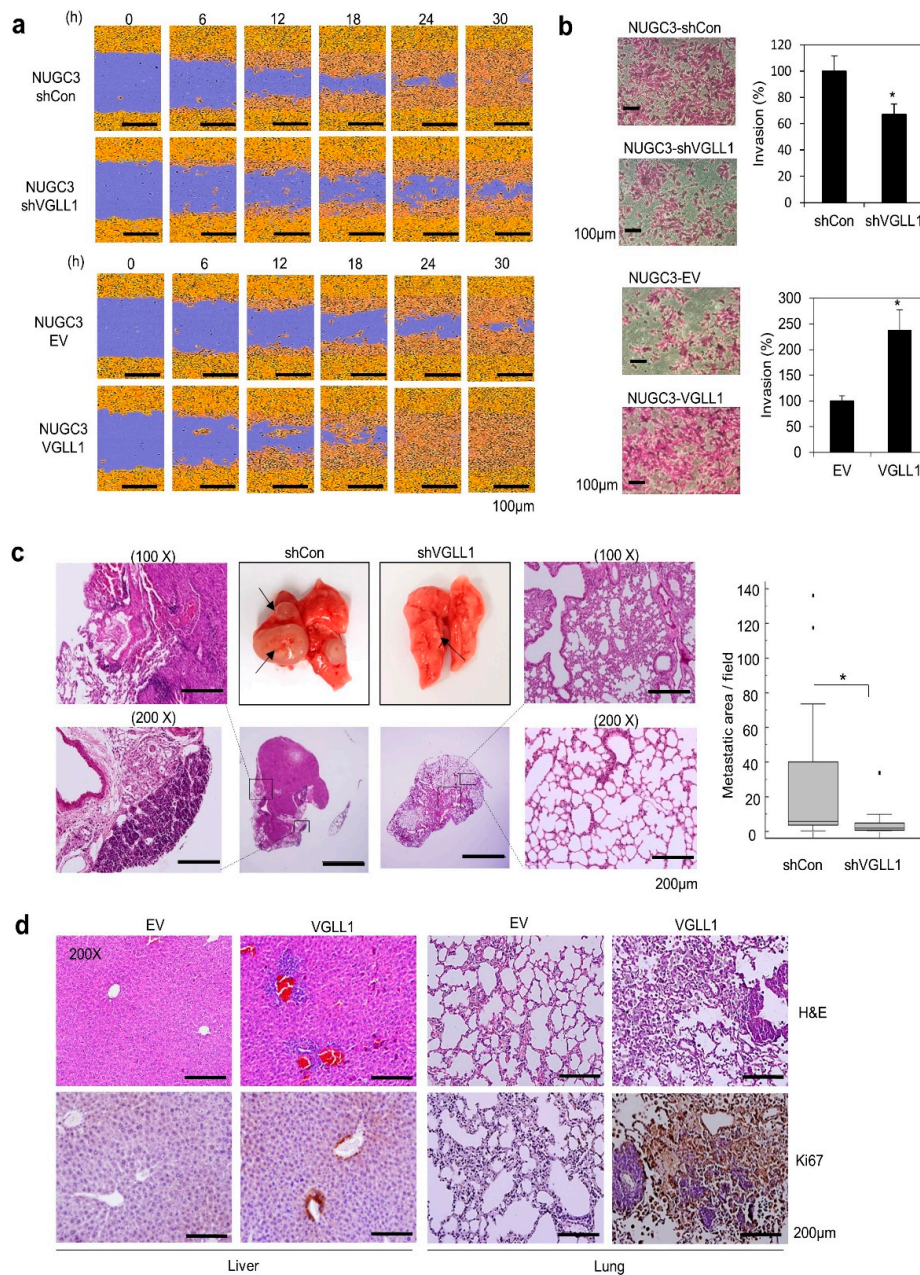


Figure 3. *VGLL1* is involved in gastric cancer metastasis. (a) Wound healing assay with *VGLL1* overexpression or knockdown in NUGC3 cells. Representative images of scratch wounds at the indicated times. (b) Invasion assays with *VGLL1*-expressing or knocked down NUGC3 cells incubated for 40 or 48 h, respectively. $n = 3$; $* p < 0.05$ (Student's *t*-test). (c) Tail vein injection assay of NUGC3 cells expressing sh*VGLL1*. H&E staining images of the lungs removed at 16 weeks after injection. The graph indicates the size of metastatic lesions ($n = 12$). Scale bar, 200 µm. $* p < 0.05$ (Student's *t*-test). (d) In vivo metastasis assay by surgical resection of *VGLL1*-expressing NUGC3 cell tumors. The liver and lungs obtained from mice sacrificed at 29 days after surgical resection of tumors formed using *VGLL1*-expressing NUGC3 cells. H&E staining and IHC staining for Ki-67 in the liver and lungs. Scale bar, 200 µm.

2.4. PI3K/AKT/ β -Catenin Signaling Participates in the Regulation of *VGLL1* Expression

Microarray analyses revealed correlations between *VGLL1* expression and PIK3CA and PIK3CB levels (Figure 1g). We also found that reducing the expression of PIK3CA or PIK3CB suppressed *VGLL1* mRNA levels (Figure 4a). LY294002, a class I PI3K inhibitor, downregulated *VGLL1* mRNA and protein levels in a dose-dependent manner in gastric cancer cell lines (Figure 4b–d). Interestingly,

LY294002 inhibited the transcription of *VGLL1*, but not that of *VGLL4* or *YAP1*, indicating the *VGLL1*-specific regulation by PI3K/AKT signaling (Figure 4d). In addition, LY294002 blocked AKT phosphorylation, thereby suppressing β -catenin (Figure 4e). Importantly, transient expression of constitutively active AKT containing S473D/T308D double mutation rescued *VGLL1* expression in the presence of LY294002 (Figure 4f), which suggested that PI3K/AKT signaling regulates *VGLL1* transcription in gastric cancer cells.

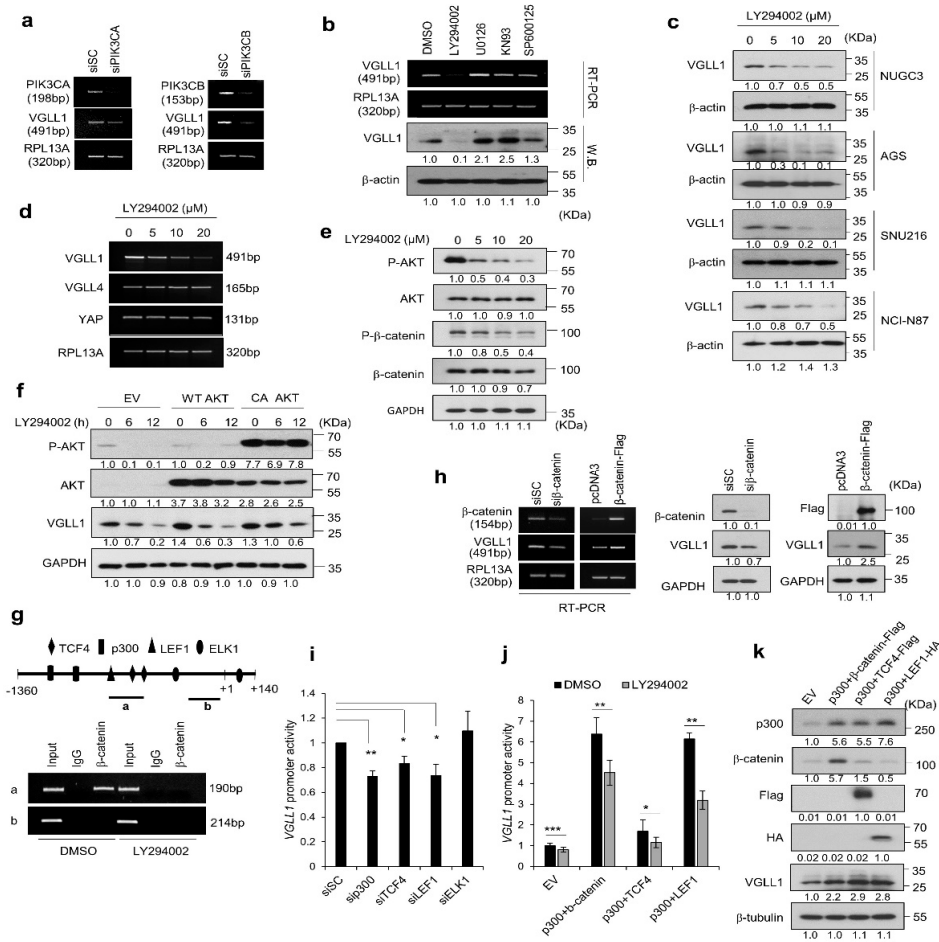


Figure 4. *VGLL1* expression is regulated by the PI3K/Akt/ β -catenin pathway. (a) Expression of *VGLL1* mRNA after treatment with siPIK3CA or siPIK3CB. (b) NUGC3 cells incubated with inhibitors (10 μ M) for 24 h. The mRNA and protein expression of *VGLL1* was analyzed by RT-PCR and western blotting, respectively. (c) Effects of LY294002 on *VGLL1* expression in gastric cancer cells. (d) mRNA levels of *VGLL1*, *VGLL4*, and *YAP* in NUGC3 cells treated with LY294002 and analyzed by RT-PCR. (e) NUGC3 cells incubated with LY294002 for 6 h at the indicated concentrations. Expression of the proteins was analyzed by western blotting. (f) Effect of AKT on *VGLL1* expression assessed by western blotting. NUGC3 cells expressing wild-type (WT) AKT or constitutively active (CA) AKT were treated with LY294002. (g) Localization of β -catenin to the *VGLL1* promoter. ChIP assay was performed using nuclear extracts of NUGC3 cells treated with LY294002. The ChIP-enriched DNA was subjected to PCR. (h) Effect of β -catenin expression knockdown or overexpression on *VGLL1* expression in NUGC3 cells analyzed by RT-PCR and western blotting. (i) *VGLL1*-promoter-driven luciferase reporter activity. NUGC3 cells were treated with siRNAs and then transfected with *VGLL1*-luc and Renilla-luc vectors. (j) Effect of LY294002 on *VGLL1* promoter activity. NUGC3 cells were co-transfected with β -catenin, p300, TCF4, LEF1, *VGLL1*-luc, and Renilla-luc for 24 h and then incubated with 10 μ M LY294002 for 24 h. Mean \pm SD of three independent experiments with triplicate measurements. * $p < 0.05$, ** $p < 0.01$, *** $p < 0.005$ (Student's *t*-test). (k) The effects of β -catenin, p300, TCF4, and LEF1 on *VGLL1* expression, assessed by western blotting.

We performed an analysis of the VGLL1 promoter to understand the mechanism underlying the transcriptional activation of VGLL1. The VGLL1 promoter contains the consensus sequences of binding sites for TCF4, LEF1, p300, and ELK1 (Figure 4g). β -catenin forms a complex with LEF/TCF for the transcriptional activation of target genes. The ChIP assay showed that β -catenin bound to the region containing LEF1 and TCF4 binding sites of the VGLL1 promoter. As expected, LY294002 treatment reduced the binding of β -catenin to the VGLL1 promoter, implicating PI3K/AKT/ β -catenin signaling for the transcription of VGLL1 (Figure 4g). VGLL1 expression was regulated by both the knockdown and overexpression of β -catenin (Figure 4h). Promoter activity was inhibited by knockdown of TCF4, LEF1, or p300 (Figure 4i). In contrast, VGLL1 promoter activity and expression were significantly increased with the co-expression of β -catenin/p300 or p300/LEF1 (Figure 4j,k). These results suggested that the β -catenin/p300/TCF4/LEF1 complex regulates VGLL1 expression at the transcription level, which acts downstream of PI3K/AKT.

2.5. VGLL1, a TEAD4 Cofactor, Regulates MMP9 Transcription

We conducted a microarray analysis of VGLL1 siRNA-treated NUGC3 cells to understand the downstream regulation of VGLL1 (Supplementary Figure S3). It seems that VGLL1 regulates various genes that are involved in cell surface receptor-linked signal transduction, immune response, cell adhesion, wound healing, and cell migration (Supplementary Figure S2b–d).

We selected MMP9 as a potential VGLL1-targeted gene, because high MMP expression is correlated with metastasis and poor prognosis in gastric cancer [24,25]. We found that MMP9 knockdown inhibited the proliferation and metastasis of NUGC3 cells (Figure 5a,b). VGLL1 knockdown reduced the MMP9 mRNA levels in NUGC3, AGS, and NCI-N87 cells (Figure 5c). MMP9 protein level was reduced by VGLL1 knockdown and increased by VGLL1 overexpression (Figure 5d). The MMP9 protein level was increased in metastasis-bearing liver and lung tissue samples in the VGLL1-overexpressing xenograft mouse model (Figure 5e).

We found two TEA sites at positions –1030 and –571, for binding of TEAD4 to the MMP9 promoter (–1295 to +1), and thus generated luciferase reporter systems with MMP9 promoters containing the wild-type TEA, deleted TEA (dTEA), and mutated TEA sites (mTEA at –571) (Figure 5f). The degree of MMP9 promoter activation was similar between the –1295 and –657 constructs, which indicated that the –1030 TEA site is not crucial in the binding of VGLL1 to TEAD4. Deletion or mutation of the TEA site at –571 resulted in significantly reduced MMP9 promoter activity (Figure 5g). TEAD4 knockdown decreased the VGLL1-induced MMP9 promoter activity (Figure 5h), which suggested that MMP9 expression coordinates TEAD4 and VGLL1 activity.

We then assessed whether the interaction between VGLL1 and TEAD4 occurred at the TEA sites in the MMP9 promoter. Interaction between VGLL1 and TEAD4 was observed by immunoprecipitation assays (Figure 5i). In chromatin immunoprecipitation (ChIP) assay, VGLL1 and TEAD4 both bound to the TEA region (a) but not to the control (b) (Figure 5j). However, in siTEAD4-treated cells, VGLL1 did not bind to the (a) region, indicating that TEAD4 is required for the binding of VGLL1 to the MMP9 promoter. These data indicate that VGLL1 functions as a cofactor of TEAD4, which binds to the TEA site at –571 in the MMP9 promoter.

Next, we asked whether YAP affects MMP9 transcription. The transient overexpression of VGLL1 increased MMP9, but not CTGF mRNA levels (Figure 5k). Likewise, the transient overexpression of YAP increased CTGF but not MMP9 mRNA levels, which suggests that YAP-independent MMP9 expression occurs in NUGC3 cells.

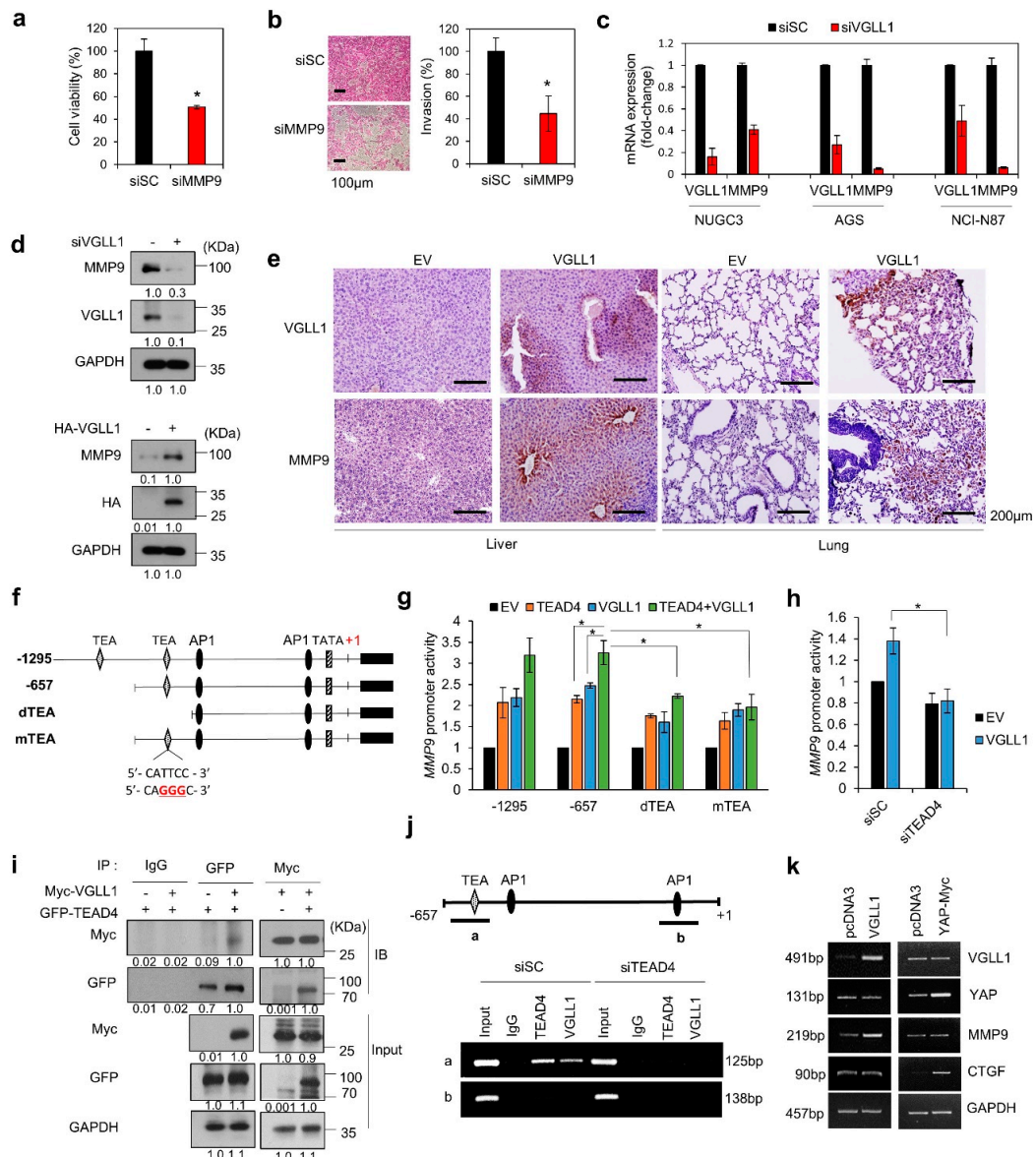


Figure 5. VGLL1 regulates *MMP9* transcription in gastric cancer cells. **(a,b)** Viability **(a)** and invasion **(b)** assay of NUGC3 cells. Cells were treated with 20 nM siScramble (SC) or siMMP9 for 48 h, and then stained with sulforhodamine B. Data are presented as mean \pm SD. $n = 3$; * $p < 0.05$ (Student's *t*-test). **(c)** *MMP9* mRNA expression regulation by VGLL1 in gastric cancer cells treated with siVGLL1 or siSC (control) was measured by qPCR. **(d)** Changes in *MMP9* expression upon knockdown or overexpression of VGLL1 assayed by western blotting in NUGC3 cells. **(e)** IHC of VGLL1 and *MMP9* expression in the liver and lungs of an in vivo metastasis mouse model using surgical resection of tumors. Scale bar, 200 μ m. **(f)** Construction of various luciferase reporter systems under control of the *MMP9* promoter. **(g)** *MMP9* promoter activities of the reporter systems containing modified TEA-binding sites were measured in NUGC3 cells. $n = 3$; * $p < 0.05$ (Student's *t*-test). **(h)** Effect of TEAD4 on VGLL1-regulated *MMP9* transcriptional activity. NUGC3 cells treated with siSC or siTEAD4 for 24 h were transfected with *MMP9*-luc, Renilla-luc, pcDNA3.1, and pcDNA3.1-myc-VGLL1 vectors for 48 h. $n = 3$; * $p < 0.05$ (Student's *t*-test). **(i)** Interaction between VGLL1 and TEAD4. Lysates of NUGC3 cells that were transfected with pcDNA3.1-myc-VGLL1 and pEGFP-N1-TEAD4 were immunoprecipitated using anti-IgG, anti-GFP, and anti-Myc antibodies. Protein expression was analyzed by immunoblotting. **(j)** ChIP assays while using nuclear extracts of NUGC3 cells treated with siTEAD4. The ChIP-enriched DNA was subjected to PCR. **(k)** Target genes of VGLL1 and YAP. NUGC3 cells were transfected with pcDNA3, pcDNA3-myc-VGLL1, or pcDNA3-myc-YAP, and the mRNA expression levels were analyzed by RT-PCR.

3. Discussion

The Hippo signaling pathway suppresses the proliferation and metastasis of cancer cells by negatively controlling YAP and TAZ, which are cofactors of TEAD transcription factors. The structural similarities between VGLL1 and YAP or TAZ suggest the formation of VGLL1–TEAD complex for cancer malignancy [21]. However, the molecular mechanism of VGLL1 in cancer is still poorly characterized. Here, we present the regulation mechanism of *VGLL1* to induce MMP9 expression that promotes gastric cancer malignancy (Figure 6).

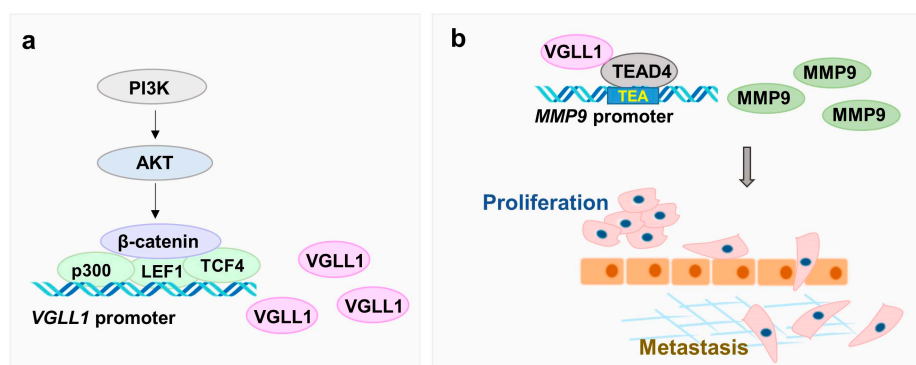


Figure 6. Cell proliferation and metastasis of gastric cancer by modulation of VGLL1 expression and activity. (a) Transcription of VGLL1 is regulated by the PI3K/AKT/β-catenin pathway. (b) VGLL1 formed complex with TEAD4 to activate transcription of MMP9, a target gene of VGLL1.

Genetic alterations in the *EGFR*, *MET*, *ERBB2*, and the *PI3K/AKT* pathway are often observed in gastric cancer. *PIK3CA* is the most mutated PI3K isoform, with an 18% mutation and 5% amplification frequency in gastric cancer [26]. Microarray analysis of gastric cancer patient tissues revealed that *VGLL1* was a prognostic biomarker and its expression was highly correlated with that of *PIK3CA* or *PIK3CB*. Moreover, a high expression of *VGLL1* and *PIK3CA* predicted worse OS in gastric cancer patients.

We observed that VGLL1 promoted the proliferation and tumorigenesis of gastric cancer cells in *in vitro* cell culture and *in vivo* xenograft mouse models. Importantly, shVGLL1-expressing NUGC3 cells suppressed lung metastasis in a mouse model, implying a crucial role of VGLL1 in cancer metastasis.

We revealed that PI3K/AKT signaling was involved in the regulation of *VGLL1* transcription. Promoter analysis demonstrated that the β-catenin/p300/TCF4/LEF1 complex induces the transcription of *VGLL1*. MMP9 was explored as a potential candidate target genes of VGLL1, because it has been reported as a molecular marker of metastasis in gastric cancer [24,25,27]. VGLL1 interacted with TEAD4 at the −571 TEA site in the *MMP9* promoter. The MMP9 levels were elevated in metastasized cancer cells in the lungs and liver in a *VGLL1*-overexpressing NUGC3 xenograft model. The MMPs, a family of zinc containing enzymes, degrade components of the extracellular matrix and regulate extracellular matrix turnover, as well as cancer processes, such as proliferation, angiogenesis, and tumor metastasis [27,28]. Interestingly, MMP9 mainly promotes tumor invasion and metastasis, while TIMP-1 inhibits the functions of MMP9 in gastric cancer, which suggests that the imbalance between MMP9 and TIMP-1 expression may occur in tumor progression [25]. We will further investigate the relationship between VGLL1 and TIMP.

Reportedly, the amino acid sequences SVIFT/HQIVHV of β2 at interface I and the VxxHF/LxxLF motif at interface II of VGLL1/YAP interact with TEAD4 to drive the expression of target genes [21,29]. Interestingly, we observed that VGLL1 regulated only *MMP9* mRNA expression, whereas YAP only regulated *CTGF* mRNA expression in NUGC3 cells. Moreover, cell proliferation promoted by *VGLL1* overexpression was not affected by *YAP* overexpression or knockdown (Supplementary Figure S4), which indicated that VGLL1 and YAP1 independently induced transcription of their target genes. Therefore, it is likely that the TEAD4–VGLL1 and TEAD4–YAP complexes use their distinctive transcriptional machineries.

Several inhibitors of the YAP–TEAD4 complex binding have been reported. Flufenamic acid, which binds the central pocket of the YAP-binding domain of TEAD2, inhibits the proliferation and migration of cancer cell [22]. Verteporfin, which disrupts the YAP–TEAD complex, is found to increase the sensitivity to paclitaxel in HCT-8/T cells [30], as well as sensitivity to erlotinib in lung cancer cells [31]. Likewise, the disruption of TEAD–VGLL1 interactions might be of use in development of anticancer drugs.

In this study, we discovered *VGLL1* as a novel prognostic biomarker correlated with *PIK3CA* or *PIK3CB* in gastric cancer. We elucidated the molecular mechanism underlying the regulation of *VGLL1* transcription by the PI3K/AKT/ β -catenin. The formation of the VGLL1–TEAD4 complex activates the transcription of *MMP9*, which then promotes proliferation and metastasis in gastric cancer cells. Taken together, we clearly elucidated the molecular mechanism that involves *VGLL1* that promotes malignancy in gastric cancer, thus suggesting *VGLL1* as a therapeutic target in treatment of gastric cancer.

4. Materials and Methods

4.1. Reagents

U0126, LY294002, KN93, SP600125, were purchased from Sigma-Aldrich (St. Louis, MO, USA). TGF- β was purchased from Peprotech (Seoul, Korea).

4.2. Cell Culture

Human gastric cancer cells (NUGC3, AGS, NCI-N87, SNU1, SNU5, SNU16, SNU216, SNU484, SNU668, Hs746T, and MKN28 cells) were cultured in RPMI-1640 medium that contained 10% fetal bovine serum (FBS). NUGC3 cells constitutively expressing *VGLL1* (NUGC3-*VGLL1* cells) were selected with 500 μ g/mL geneticin (Thermo Scientific, Logan, UT, USA). HEK293T cells were cultured in Dulbecco's modified Eagle's medium (DMEM) containing 10% FBS. All the cells were cultured in an atmosphere of 5% CO₂ at 37 °C. STR profiling by Korea Cell Line Bank authenticated all of the cell lines (Seoul, Korea).

4.3. Patients

A retrospective review of a gastric cancer cohort database prospectively maintained at Yonsei University College of Medicine (Seoul, South Korea) was conducted to identify all the gastric adenocarcinoma patients who underwent curative D2 gastrectomy between 2000 and 2010. Demographic and clinicopathological information and tumor tissue samples were obtained from 556 patients. The institutional review board of Severance Hospital approved this study (Seoul, Korea; 2015-3104-001).

4.4. Microarray Experiments and Data Processing

The total RNA extracted from 556 gastric cancer tissues was used for labeling and hybridization, according to the manufacturer's protocols (Illumina HumanWG-6 BeadChip, version 2, Illumina, San Diego, CA, USA). The arrays were scanned with an Illumina Bead Array Reader confocal scanner (BeadStation 500GXDW; Illumina, Inc., San Diego, CA, USA), as per the manufacturer's instructions. After scanning, the microarray data were log₂ transformed, median centered across genes and samples, and normalized while using quantile normalization in the R language environment (version 3.2.5, The R Foundation for Statistical Computing, Vienna, Austria). The microarray data set of gastric cancer samples from patients is available in the NCBI Database of GEO datasets under the data series accession numbers GSE13861 and GSE84437. The microarray analysis of *VGLL1* siRNA-treated NUGC3 cells while using same procedure and microarray data set is available in the NCBI Database of GEO datasets under accession numbers GSE130071. We applied the FDR approach for analysis of microarray data. After FDR correction, we selected genes (p value < 0.05 and log₂FC > 1) for GO analysis.

4.5. Statistical Analysis of Microarray

Pearson correlation coefficients were calculated for evaluating the association between genes. We obtained an optimal cut-off for gene expression from ROC analysis to classify patients into two subgroups by single gene expression, in which the best cut-off was determined by the expression with the highest multiply of sensitivity and specificity. Statistical analyses were carried out while using Medcalc version 18.11.6 (MedCalc software, Ostend, Belgium). The Kaplan-Meier method was used to calculate the time before death or recurrence, and difference between the times was assessed using logrank test (MedCalc software, Ostend, Belgium). A gene set enrichment analysis was carried out to identify the most significant gene sets associated with molecular and cellular functions. Fisher's exact test estimated the significance of over-represented gene sets. Gene set enrichment analyses were performed using the DAVID bioinformatics resources (ver. 6.8, Laboratory of Human Retrovirology and Immunoinformatics, Frederick, MD, USA).

4.6. Plasmids Construction

pOBT7-*VGLL1* and pCMV-SPORT6-*TEAD4* were obtained from Korean UniGene Information (KUGI). *VGLL1* mRNA was amplified via PCR and then cloned into the HindIII/BamHI sites of pcDNA3.1 with Myc-tag. *TEAD4* was inserted in the HindIII/BamHI sites of pEGFP-N1. *YAP* was amplified via PCR and then cloned into the EcoRV/XbaI sites of pcDNA3.1 with Myc-tag. Fragments of the *MMP9* promoter (−657/+25, −557/+25) were PCR-amplified and subsequently inserted into the KpnI/XhoI site of pGL4.17 (Luc2/neo). The *MMP9* promoter, which contained mutation in TEA binding site (5'-CATTCC-3' → 5'-CAGGGC-3'), was generated while using the Quikchange Site-Directed Mutagenesis kit. The fragment of *VGLL1* promoter was PCR-amplified and cloned into the XhoI/HindIII site of pGL2-basic luciferase plasmid. pCMV3- β -catenin, pCMV3-*p300*, pCMV3-*TCF4*, and pCMV3-*LEF1* were obtained from Sino Biological (Wayne, PA, USA).

4.7. Live cell Assay for Cell Proliferation and Migration

Proliferation rates, which were based on cell confluence, were determined by live-cell imaging (IncuCyte ZOOM System, Essen BioScience, Ann Arbor, MI, USA), as described previously [32]. To analyze cell migration, the cells were cultured in 96-well ImageLock Plates (Essen BioScience) to reach confluence prior to wound creation. A scratch was made in confluent monolayers while using a 96-pin WoundMaker (Essen BioScience, Ann Arbor, MI, USA). The cells were washed with PBS and then incubated using the IncuCyte ZOOM system. Cell migration was analyzed at 2 h intervals throughout the duration of the experiment.

4.8. Spheroid Formation

Three-dimensional (3D)-Spheroid culture was induced, as described previously [33]. In brief, cells were trypsinized, counted, and diluted to 5×10^4 cells in a 20 μ L droplet. The droplets of cell suspension were placed on the lid of a sterile non-adherent polystyrene petri dish that was filled with DPBS, and then cultured at 37 °C in a 5% CO₂ incubator for 48 h.

4.9. Mice Experiments

The bioethics committee of the Korea Research Institute of Bioscience and Biotechnology approved all animal experiments (KRIBB-ACE-16101, KRIBB-ACE-17051, and KRIBB-ACE-18209). In vivo xenografts were performed, as described previously [32]. NUGC3 cells (5×10^6) that were infected with a lentiviral sh*VGLL1* vector were subcutaneously injected into five-week-old female BALB/c nude mice. According to the protocol that was published by Le A. [34], stable *VGLL1*-expressing HEK293T cells (1×10^7) were subcutaneously injected into five-week-old female BALB/c nude mice.

We established an in vivo xenograft mouse model to study the effect of *VGLL1* on gastric cancer metastasis. Five-week-old female nude mice (six mice per group) were subcutaneously inoculated

with NUGC3-EV or NUGC3-*VGLL1* cells (5×10^6) in the right flank. Surgical resection of the primary tumor was performed when the average tumor volume reached 500 mm^3 . After four weeks, the mice were sacrificed by cervical dislocation under isoflurane anesthesia, and lung and liver tissue was also removed for subsequent experiments. For a tail vein-injection assay of cancer metastasis, NUGC3 cells (1×10^6) cells that were infected with a lentivirus expressing shControl or sh*VGLL1* were injected into the tail vein of mice (four mice per group) in $100 \mu\text{L}$ of phosphate-buffered saline (PBS). After 16 weeks, the lungs were removed and fixed. Hematoxylin and eosin (H&E) assessed tumor metastasis to the lungs and liver. Photos of random fields were obtained at a magnification of $40\times$ (3 fields/mouse) and analyzed while using NIH Image software for the quantitation of metastasis (ver. 1.48, Wayne Rasband, Bethesda, Maryland, USA) [35].

4.10. Western Blot Analysis

The cells were lysed with RIPA buffer (Millipore, Billerica, MA, USA) containing protease inhibitor cocktail (Roche), and the lysates were quantified with a protein assay kit (Bio-Rad, Hercules, CA, USA). The cell lysates were separated using SDS-PAGE and then transferred to PVDF membranes. The proteins were identified while using appropriate antibodies. Anti-*VGLL1* (10124-2-AP) was purchased from Proteintech (Rosemont, IL, USA). Anti-*TEAD4* (ab58310) and anti-*MMP9* (ab76003) were purchased from Abcam (Cambridge, MA, USA). Anti-GFP (NB600-308) was purchased from Novus Biologicals (Centennial, CO, USA). Anti-Myc (sc-789) and anti-HA (sc-805) were purchased from Santa Cruz Biotechnology (Dallas, TX, USA). Anti-GAPDH (LF-PA0212) was purchased from AbFrontier (Seoul, Korea). Anti- β -tubulin (2128), anti-pSer473-AKT (9271), anti-AKT (9272), anti-p- β -catenin (9561), and anti- β -catenin (9562) were purchased from Cell Signaling (Danvers, MA, USA). Anti-Flag (F1804) was purchased from Sigma-Aldrich (St. Louis, MO, USA). The protein signal was detected while using an enhanced chemiluminescence kit (Millipore, Burlington, MA, USA).

4.11. Reverse Transcriptase Polymerase Chain Reaction and Quantitative Real-Time PCR

The total RNA was isolated using TRIzol reagent (Invitrogen, Carlsbad, CA, USA), and cDNA was synthesized using TOPscriptTM RT DryMIX (Enzymomics, Daejeon, Korea). RT-PCR was performed using Dr. Taq MasterMix (Doctor Protein, Daejeon, Korea). Quantitative real-time PCR was performed using a SYBR Green master mix kit (Qiagen, Valencia, CA, USA). The following sequences of primers were used: *VGLL1* (F) 5'-GAGCTGTGGCATTCTCCTC-3', (R) 5'-AAGTGGGTGTGAGCAGCTTT-3', *MMP9* (F) 5'-TCTATGGTCCTCGCCCTGAA-3', (R) 5'-CATCGTCCACCGACTCAAA-3', *TEAD4* (F) 5'-GAACGGGGACCCTCCAATG-3', (R) 5'-GCGAGCATACTCTGTCTCAAC-3', *YAP* (F) 5'-CGCTCTTCAACGCCGTC-3', (R) 5'-AGTACTGGCCTGTCCGGAGT-3', *CTGF* (F) 5'-CTTGCGAAGCTGACCTGGAA-3', (R) 5'-AAAGCTCAAACCTTGATAGGCTTGGA-3', *PIK3CA* (F) 5'-TGCAGCCATTGACCTGTTA-3', (R) 5'-GTCAAACAATGGCACACG-3', *GAPDH* (F) 5'-TCATGACCACAGTCCATGCC-3', (R) 5'-TCCACCACCCTGTTGCTGTA-3', *RPL13A* (F) 5'-CATCGTGGCTAAACAGGTAC-3', and (R) 5'-GCACGACCTTGAGGGCAGC-3'. The primers of *PIK3CB* (P144505) was purchased from Bioneer (Daejeon, Korea).

4.12. Gene Knockdown Using siRNA

Introducing siRNA into the target gene, using Lipofectamine 2000 (Invitrogen, Carlsbad, CA, USA), according to the manufacturer's instructions, was undertaken to perform gene knockdown. The siRNA sequences were, as follows: siScramble (siSC) 5'-CCUACGCCACCAAUUUCGUdTdT-3', si*VGLL1* 5'-AGCCUAUAAAGACGGAAUGGA AUdTdT-3' and 5'-CCCGGUGUGUCCUUUUCACCUACdTdT-3', si*TEAD4* 5'-GACACUACUCUACCGCAUdTdT-3', si*YAP* 5'-CCACCA AGCUAGAUA AAA GAAAdTdT-3', si*MMP9* 5'-CCACAACAUCACCUAUUGGAUdTdT-3', si*p300* 5'-GAUGAAUGCGGG CAUGAAU dTdT-3', si- β -catenin 5'-CGUUCUCCUCAGAUGGUGUdTdT-3', si*TCF4* 5'-CAGAC AAAGAAAGUUCGAAAdTdT-3', si*LEF1* 5'-GAACGACUCUGAAAUCAUCUU dTdT-3', si*PIK3CA* 5'-CUG AGAAAUGAAAGCUCACUCUdTdT-3', and si*PIK3CB* 5'-CAGUACAA UUUGGUGUCAUdTdT-3'.

4.13. Lentivirus Infection

shControl and shVGLL1 (Sigma, TRCN0000019618) were packaged into lentivirus via HEK293T cells, using Lipofectamine and PLUS Reagent (Invitrogen, Carlsbad, CA, USA), and then transduced into NUGC3 cells. Post-transduction 48 h, the NUGC3 cells were selected with puromycin (1 µg/mL).

4.14. Immunohistochemistry (IHC)

US Biomax supplied tissue array blocks of human gastric cancer and normal tissues (Rockville, MD, USA). IHC was performed, as previously described [32]. The slides were incubated with anti-VGLL1 (Proteintech, 10124-2-AP, Rosemont, IL, USA), anti-Ki67 (abcam, ab15580), and anti-MMP9 (abcam, ab76003) antibodies. After washing with PBS, the slides were incubated with biotinylated anti-rabbit IgG (Vector Laboratories, Burlingame, CA, USA) and avidin-biotin peroxidase (Vector Laboratories) and visualized using diaminobenzidine tetrahydrochloride (Vector Laboratories, Burlingame, CA, USA). The sections were counterstained with hematoxylin.

4.15. Invasion Assay

For invasion assays, chambers with 8.0-µm-pore PET membrane in 24-well cell culture inserts (BD Biosciences, San Jose, CA, USA) were used. The cells in serum-free medium were seeded into the upper part of each chamber with Matrigel coating, whereas the lower compartments were filled with the above-mentioned medium. The cells were then allowed to invade, being subsequently fixed with 10% formalin, and stained with sulforhodamine B (SRB), as previously described [36].

4.16. Luciferase Assay

A dual-luciferase reporter system determined the promoter activity (Promega, Madison, WI, USA). The cells were transfected with pGL4.17-MMP9-luciferase (MMP9-luc), pGL2-VGLL1-luciferase (VGLL1-luc), and pRL-SV40 plasmid encoding firefly (Renilla)-luciferase, using PolyFect (Qiagen, Valencia, CA, USA). The luciferase activity was measured using a luminometer (VICTOR X Light; PerkinElmer, Waltham, MA, USA). The results were normalized to the activity of Renilla luciferase.

4.17. Chromatin Immunoprecipitation (ChIP) Assays

ChIP assays were performed, as previously described [36]. Briefly, the cells were crosslinked using 1% formaldehyde and then lysed. The chromatin was then sheared via sonication on ice. The lysates were incubated with antibodies targeting β-catenin, VGLL1 or TEAD4, or with normal mouse immunoglobulin G (IgG) overnight at 4 °C. Thereafter, protein was digested using proteinase K (Millipore, Middlesex County, MA, USA). The ChIP-enriched DNA was subjected to PCR while using either of the following two primers: VGLL1-a (5'-GTA GAC AAA GAG AGG AGC-3' and 5'-GGC TTC CAT TGG CCA AAG-3'), VGLL1-b (5'-TTT GTT GTT GAC TCT GTG T-3' and 5'-AAG GCG TTT CCT GCT AGC-3'), MMP9-a (5'-TACTGTCCCCTTTACTGC-3' and 5'-CTTCCTCTCCCTGCTTCA-3'), and MMP9-b (5'-TG GTGTAAGCCCTTTCTC-3' and 5'-AGGAGGCGCTCCTGTGAC-3').

4.18. Statistical Analyses

Student's *t*-tests or Chi-square tests were used for statistical analyses. The bars indicate S.D., and the asterisks denote significant differences (** $p \leq 0.005$, * $p \leq 0.01$, * $p \leq 0.05$) between the means of two groups.

5. Conclusions

VGLL1 is a prognostic biomarker that correlates with PIK3CA and PIK3CB in gastric cancer. PI3K/AKT/β-catenin transcriptionally activates VGLL1, thus calibrating MMP9 expression linked to gastric cancer malignancy. Our finding proposes VGLL1 as a therapeutic target for malignant gastric cancer.

Supplementary Materials: The following are available online at <http://www.mdpi.com/2072-6694/11/12/1923/s1>, Figure S1: The expression of VGLL1. Figure S2: The effect of VGLL1 overexpression on the proliferation of gastric cancer cells expressing low VGLL1. Figure S3: Microarray analysis of NUGC3 cells treated with siVGLL1. Figure S4: Effect of YAP knockdown/overexpression on cell growth in NUGC3-EV and NUGC3-VGLL1 cells. Table S1: Expression of VGLL1 and clinicopathologic characteristics of 556 patients with gastric cancer.

Author Contributions: conceptualization, B.-K.K. and M.W.; J.-H.C.; funding acquisition, M.W. and B.-K.K.; investigation, B.-K.K., J.-Y.I., H.S.B., M.-J.K. and J.L.; methodology, B.-K.K. and J.-H.C.; project administration, M.-J.K.; resources, J.-H.C.; software and formal analysis, B.-K.K., S.-K.K. and S.-Y.K.; supervision, M.W.; validation, B.-K.K.; visualization, B.-K.K.; supervision, M.W.; writing—original draft preparation, B.-K.K., J.-H.C. and M.W.; writing—review and editing, K.-C.P., S.P., J.-H.C.

Funding: This work was supported by the National Research Foundation (NRF) under Grant NRF-2017R1A2B2011936, NRF-2018R1A5A2023127 and NRF-2019R1A2C1087492, Health Technology R&D Grant H113C2162 and the KRIBB Initiative program under Grant KGM4751713.

Acknowledgments: We would like to thank Kim Soo-Jin and Woo-il Kim for helping with animal experiments. We also appreciate Alexander Song (Department of Internal Medicine, Wake Forest Baptist Medical Center) for reviewing the manuscript.

Conflicts of Interest: The authors declare no conflict of interest.

References

- Cheong, J.H.; Yang, H.K.; Kim, H.; Kim, W.H.; Kim, Y.W.; Kook, M.C.; Park, Y.K.; Kim, H.H.; Lee, H.S.; Lee, K.H.; et al. Predictive test for chemotherapy response in resectable gastric cancer: A multi-cohort, retrospective analysis. *Lancet Oncol.* **2018**, *19*, 629–638. [[CrossRef](#)]
- Kelly, C.M.; Janjigian, Y.Y. The genomics and therapeutics of HER2-positive gastric cancer—from trastuzumab and beyond. *J. Gastrointest. Oncol.* **2016**, *7*, 750–762. [[CrossRef](#)] [[PubMed](#)]
- Grabsch, H.; Sivakumar, S.; Gray, S.; Gabbert, H.E.; Muller, W. HER2 expression in gastric cancer: Rare, heterogeneous and of no prognostic value—conclusions from 924 cases of two independent series. *Cell Oncol.* **2010**, *32*, 57–65.
- Boku, N. HER2-positive gastric cancer. *Gastric Cancer* **2014**, *17*, 1–12. [[CrossRef](#)] [[PubMed](#)]
- Apicella, M.; Corso, S.; Giordano, S. Targeted therapies for gastric cancer: Failures and hopes from clinical trials. *Oncotarget* **2017**, *8*, 57654–57669. [[CrossRef](#)]
- Li, K.; Li, J. Current Molecular Targeted Therapy in Advanced Gastric Cancer: A Comprehensive Review of Therapeutic Mechanism, Clinical Trials, and Practical Application. *Gastroenterol. Res. Pract.* **2016**, *2016*, 4105615. [[CrossRef](#)]
- Baniak, N.; Senger, J.L.; Ahmed, S.; Kanthan, S.C.; Kanthan, R. Gastric biomarkers: A global review. *World J. Surg. Oncol.* **2016**, *14*, 212. [[CrossRef](#)]
- Wong, H.; Yau, T. Molecular targeted therapies in advanced gastric cancer: Does tumor histology matter? *Therap. Adv. Gastroenterol.* **2013**, *6*, 15–31. [[CrossRef](#)]
- Wang, K.; Yuen, S.T.; Xu, J.; Lee, S.P.; Yan, H.H.; Shi, S.T.; Siu, H.C.; Deng, S.; Chu, K.M.; Law, S.; et al. Whole-genome sequencing and comprehensive molecular profiling identify new driver mutations in gastric cancer. *Nat. Genet.* **2014**, *46*, 573–582. [[CrossRef](#)] [[PubMed](#)]
- Tan, P.; Yeoh, K.G. Genetics and Molecular Pathogenesis of Gastric Adenocarcinoma. *Gastroenterology* **2015**, *149*, 1153–1162.e3. [[CrossRef](#)] [[PubMed](#)]
- Jacome, A.A.; Coutinho, A.K.; Lima, E.M.; Andrade, A.C.; Dos Santos, J.S. Personalized medicine in gastric cancer: Where are we and where are we going? *World J. Gastroenterol.* **2016**, *22*, 1160–1171. [[CrossRef](#)] [[PubMed](#)]
- Samuels, Y.; Diaz, L.A. Jr.; Schmidt-Kittler, O.; Cummins, J.M.; DeLong, L.; Cheong, I.; Rago, C.; Huso, D.L.; Lengauer, C.; Kinzler, K.W.; et al. Mutant PIK3CA promotes cell growth and invasion of human cancer cells. *Cancer Cell* **2005**, *7*, 561–573. [[CrossRef](#)] [[PubMed](#)]
- Nakanishi, Y.; Walter, K.; Spoerke, J.M.; O'Brien, C.; Huw, L.Y.; Hampton, G.M.; Lackner, M.R. Activating Mutations in PIK3CB Confer Resistance to PI3K Inhibition and Define a Novel Oncogenic Role for p110beta. *Cancer Res.* **2016**, *76*, 1193–1203. [[CrossRef](#)] [[PubMed](#)]
- Vaudin, P.; Delanoue, R.; Davidson, I.; Silber, J.; Zider, A. TONDU (TDU), a novel human protein related to the product of vestigial (vg) gene of *Drosophila melanogaster* interacts with vertebrate TEF factors and substitutes for Vg function in wing formation. *Development* **1999**, *126*, 4807–4816.

15. Zhou, Y.; Huang, T.; Cheng, A.S.; Yu, J.; Kang, W.; To, K.F. The TEAD Family and Its Oncogenic Role in Promoting Tumorigenesis. *Int. J. Mol. Sci.* **2016**, *17*, 138. [[CrossRef](#)]
16. Lamar, J.M.; Stern, P.; Liu, H.; Schindler, J.W.; Jiang, Z.G.; Hynes, R.O. The Hippo pathway target, YAP, promotes metastasis through its TEAD-interaction domain. *Proc. Natl. Acad. Sci. USA* **2012**, *109*, E2441–E2450. [[CrossRef](#)]
17. Lim, B.; Park, J.L.; Kim, H.J.; Park, Y.K.; Kim, J.H.; Sohn, H.A.; Noh, S.M.; Song, K.S.; Kim, W.H.; Kim, Y.S.; et al. Integrative genomics analysis reveals the multilevel dysregulation and oncogenic characteristics of TEAD4 in gastric cancer. *Carcinogenesis* **2014**, *35*, 1020–1027. [[CrossRef](#)]
18. Zhang, W.; Gao, Y.; Li, P.; Shi, Z.; Guo, T.; Li, F.; Han, X.; Feng, Y.; Zheng, C.; Wang, Z.; et al. VGLL4 functions as a new tumor suppressor in lung cancer by negatively regulating the YAP-TEAD transcriptional complex. *Cell Res.* **2014**, *24*, 331–343. [[CrossRef](#)]
19. Jiao, S.; Wang, H.; Shi, Z.; Dong, A.; Zhang, W.; Song, X.; He, F.; Wang, Y.; Zhang, Z.; Wang, W.; et al. A peptide mimicking VGLL4 function acts as a YAP antagonist therapy against gastric cancer. *Cancer Cell* **2014**, *25*, 166–180. [[CrossRef](#)]
20. Zhang, Y.; Shen, H.; Withers, H.G.; Yang, N.; Denson, K.E.; Mussell, A.L.; Truskinovsky, A.; Fan, Q.; Gelman, I.H.; Frangou, C.; et al. VGLL4 Selectively Represses YAP-Dependent Gene Induction and Tumorigenic Phenotypes in Breast Cancer. *Sci. Rep.* **2017**, *7*, 6190. [[CrossRef](#)]
21. Pobbati, A.V.; Chan, S.W.; Lee, I.; Song, H.; Hong, W. Structural and functional similarity between the Vgll1-TEAD and the YAP-TEAD complexes. *Structure* **2012**, *20*, 1135–1140. [[CrossRef](#)] [[PubMed](#)]
22. Pobbati, A.V.; Han, X.; Hung, A.W.; Weiguang, S.; Huda, N.; Chen, G.Y.; Kang, C.; Chia, C.S.; Luo, X.; Hong, W.; et al. Targeting the Central Pocket in Human Transcription Factor TEAD as a Potential Cancer Therapeutic Strategy. *Structure* **2015**, *23*, 2076–2086. [[CrossRef](#)] [[PubMed](#)]
23. Castilla, M.A.; Lopez-Garcia, M.A.; Atienza, M.R.; Rosa-Rosa, J.M.; Diaz-Martin, J.; Pecero, M.L.; Vieites, B.; Romero-Perez, L.; Benitez, J.; Calcabrini, A.; et al. VGLL1 expression is associated with a triple-negative basal-like phenotype in breast cancer. *Endocr. Relat. Cancer* **2014**, *21*, 587–599. [[CrossRef](#)] [[PubMed](#)]
24. Chen, S.Z.; Yao, H.Q.; Zhu, S.Z.; Li, Q.Y.; Guo, G.H.; Yu, J. Expression levels of matrix metalloproteinase-9 in human gastric carcinoma. *Oncol. Lett.* **2015**, *9*, 915–919. [[CrossRef](#)]
25. Zhang, S.; Li, L.; Lin, J.Y.; Lin, H. Imbalance between expression of matrix metalloproteinase-9 and tissue inhibitor of metalloproteinase-1 in invasiveness and metastasis of human gastric carcinoma. *World J. Gastroenterol.* **2003**, *9*, 899–904. [[CrossRef](#)]
26. Tran, P.; Nguyen, C.; Klempner, S.J. Targeting the Phosphatidylinositol-3-kinase Pathway in Gastric Cancer: Can Omics Improve Outcomes? *Int. Neurolog. J.* **2016**, *20* (Suppl. S2), S131–S140. [[CrossRef](#)]
27. Deryugina, E.I.; Quigley, J.P. Matrix metalloproteinases and tumor metastasis. *Cancer Metastasis Rev.* **2006**, *25*, 9–34. [[CrossRef](#)]
28. Kessenbrock, K.; Plaks, V.; Werb, Z. Matrix metalloproteinases: Regulators of the tumor microenvironment. *Cell* **2010**, *141*, 52–67. [[CrossRef](#)]
29. Mesrouze, Y.; Hau, J.C.; Erdmann, D.; Zimmermann, C.; Fontana, P.; Schmelzle, T.; Chene, P. The surprising features of the TEAD4-Vgll1 protein-protein interaction. *Chembiochem* **2014**, *15*, 537–542. [[CrossRef](#)]
30. Pan, W.; Wang, Q.; Zhang, Y.; Zhang, N.; Qin, J.; Li, W.; Wang, J.; Wu, F.; Cao, L.; Xu, G. Verteporfin can Reverse the Paclitaxel Resistance Induced by YAP Over-Expression in HCT-8/T Cells without Photoactivation through Inhibiting YAP Expression. *Cell Physiol. Biochem.* **2016**, *39*, 481–490. [[CrossRef](#)]
31. Hsu, P.C.; You, B.; Yang, Y.L.; Zhang, W.Q.; Wang, Y.C.; Xu, Z.; Dai, Y.; Liu, S.; Yang, C.T.; Li, H.; et al. YAP promotes erlotinib resistance in human non-small cell lung cancer cells. *Oncotarget* **2016**, *7*, 51922–51933. [[CrossRef](#)] [[PubMed](#)]
32. Kim, B.K.; Nam, S.W.; Min, B.S.; Ban, H.S.; Paik, S.; Lee, K.; Im, J.Y.; Lee, Y.; Park, J.T.; Kim, S.Y.; et al. Bcl-2-dependent synthetic lethal interaction of the IDF-11774 with the V0 subunit C of vacuolar ATPase (ATP6V0C) in colorectal cancer. *Br. J. Cancer* **2018**, *119*, 1347–1357. [[CrossRef](#)] [[PubMed](#)]
33. Kelm, J.M.; Timmins, N.E.; Brown, C.J.; Fussenegger, M.; Nielsen, L.K. Method for generation of homogeneous multicellular tumor spheroids applicable to a wide variety of cell types. *Biotechnol. Bioeng.* **2003**, *83*, 173–180. [[CrossRef](#)] [[PubMed](#)]
34. Le, A.; Stine, Z.E.; Nguyen, C.; Afzal, J.; Sun, P.; Hamaker, M.; Siegel, N.M.; Gouw, A.M.; Kang, B.H.; Yu, S.H.; et al. Tumorigenicity of hypoxic respiring cancer cells revealed by a hypoxia-cell cycle dual reporter. *Proc. Natl. Acad. Sci. USA* **2014**, *111*, 12486–12491. [[CrossRef](#)] [[PubMed](#)]

35. Takeda, Y.; Li, Q.; Kazarov, A.R.; Epardaud, M.; Elpek, K.; Turley, S.J.; Hemler, M.E. Diminished metastasis in tetraspanin CD151-knockout mice. *Blood* **2011**, *118*, 464–472. [[CrossRef](#)] [[PubMed](#)]
36. Kim, B.K.; Im, J.Y.; Han, G.; Lee, W.J.; Won, K.J.; Chung, K.S.; Lee, K.; Ban, H.S.; Song, K.; Won, M. p300 cooperates with c-Jun and PARP-1 at the p300 binding site to activate RhoB transcription in NSC126188-mediated apoptosis. *Biochim. Biophys. Acta* **2014**, *1839*, 364–373. [[CrossRef](#)] [[PubMed](#)]



© 2019 by the authors. Licensee MDPI, Basel, Switzerland. This article is an open access article distributed under the terms and conditions of the Creative Commons Attribution (CC BY) license (<http://creativecommons.org/licenses/by/4.0/>).